Ultrafast Coherent Transients & Excited State Dynamics in Gases and Solids

Thesis by

Daniel Richard Dawson

In Partial Fulfillment of the Requirements for the Degree of

Master of Science

California Institute of Technology

Pasadena, California

1978

(submitted June 1977)

Abstract

I. A new technique utilizing the electro-optic frequency switching of a single mode (6 Mhz) dye laser was used to observe free induction decay and optical nutation in iodine gas and optical nutation in an organic mixed crystal (pentacene in p-terphenyl) at low temperature. A new technique, incoherent resonance decay (IRD) was also developed. These experiments allow one to determine T_1 and T_2, the longitudinal and transverse relaxation times of the excited ensemble, in analogy with magnetic resonance. For $I_{2(g)}$ at 0°C; $T_1 = 2.3 \times 10^{-7}$ sec, $T_2 \simeq 1 \times 10^{-7}$ sec. These techniques are limited to a time scale >10 nsec.

II. The construction and characterization of "cw", mode-locked dye laser capable of putting out a continuous train of reproducible sub-picosecond pulses is described. Experiments utilizing this laser for the measurement of picosecond coherent transients and time resolved absorption spectroscopy are proposed.

Table of Contents

		Page
I.	Nanosecond Coherent Transients	
	A. Introduction	1
	B. Experimental	6
	C. Demonstration of Coherent Transients in Gases and Solids	10
II.	Picosecond Coherent Transients and Time Resolved Absorption Spectroscopy	
	A. Introduction	13
	B. Experimental	16
	C. Proposed Experiments	28
III.	References	42

I. Nanosecond Coherent Transients

A. Introduction

The observation of coherent transients, fast or shortlived transient signals due to interference between coherently prepared ensembles, dates back to 1950 when Hahn[1] demonstrated the refocusing of an oscillating, macroscopic spin magnetic moment in his classical spin echo experiment. These experiments allow one to determine the so-called transverse relaxation time T_2, the 1/e time for the loss of phase coherence. As any observable property such as the bulk magnetization in magnetic resonance is necessarily an ensemble average over the individual spins, both the lifetime (T_1) and the phase (T_2) of the spins are important.

In the optical regions the question with which we have concerned ourselves focuses on the time evolution of a "primary" state following absorption. Historically, the observed lifetime as well as the width and shape of optical resonances has comprised the available information. We now know that in most cases these resonances are inhomogeneously broadened. That is, the optical resonance observed with an absorption spectrum does not reflect the true homogeneous linewidth of a molecule as determined by the various decay channels. Rather, the line is broadened due to the fact that various homogeneously broadened ensembles see slightly different environments leading to small variations in their resonant frequencies. This can be due to the doppler effect in gases or the so-called strain broadening in solids.

To fully understand the decay of an excited ensemble, one must know the true homogeneous linewidth. In addition, one would like to sort out

accurately the various contributions to the broadening from decay channels (optical T_1 properties) as well as dephasing of the molecular transition dipoles in the excited ensemble. What we desired was a fairly routine optical measurement that could yield both T_1 and T_2 information for a variety of systems. As will be shown, the techniques developed also allow us to extract μ, the transition dipole moment.

In 1964 Kurnit et al.[2] demonstrated the photon echo, the optical analog of Hahn's experiment. Rather than working with permanent nuclear spin moment, in the optical region one works with the transition dipole moment formed from a coherent superposition of states.

Consider coherent excitation of a two-level system yielding a superposition of the two states

$$\psi(r,t) = C_g\, e^{-\omega_g t}\psi_g(r) + C_e\, e^{-\omega_e t}\psi_e(r) \tag{1}$$

where subscripts g and e denote the ground and excited states respectively and $\omega \equiv E/\hbar$. The expectation value for the moment μ, assuming neither state has a permanent dipole moment, is given by

$$\langle\mu\rangle = \langle\psi(r_1 t)|\mu|\psi(r_1 t)\rangle = C_g C_e^* \mu_{ge}\, e^{i\omega_o t} + \text{c.c.} \tag{2}$$

where $\omega_o = \omega_e - \omega_g$ and $\mu_{ge} \equiv \langle\psi_g(r)|\mu|\psi_e(r)\rangle$. This pure state can be represented with the density matrix formalism as

$$\underset{\approx}{\rho} = \begin{pmatrix} C_g C_g^* & C_g C_e^* e^{i\omega_o t} \\ C_g^* C_e\, e^{-i\omega_o t} & C_e C_e^* \end{pmatrix} = \begin{pmatrix} \rho_{gg} & \rho_{ge} \\ \rho_{eg} & \rho_{ee} \end{pmatrix} \tag{3}$$

Now consider the interaction V(t) such that the hamiltonian for the system is

$$H = H_o + V(t) \tag{4}$$

Using the equation of motion we can show the rate of change of the elements of the density matrix are given by

$$-\dot{\rho}_{aa} = \frac{-i}{\hbar}(V_{ab}\rho_{ba} - V_{ba}\rho_{ab}) \tag{5a}$$

$$-\dot{\rho}_{bb} = \frac{i}{\hbar}(V_{ab}\rho_{ba} - V_{ba}\rho_{ab}) \tag{5b}$$

$$-\dot{\rho}_{ab} = \frac{-i}{\hbar}(\rho_{aa} - \rho_{bb})V_{ab} \tag{5c}$$

Defining, in analogy with magnetic resonance, phenomenalogical decay constants T_a and T_b, and dipole dephasing time constant T_2, we write

$$-\dot{\rho}_{aa} = \rho_{aa}/T_{1a} - \frac{i}{\hbar}(V_{ab}\rho_{ba} - V_{ba}\rho_{ab}) \tag{6a}$$

$$-\dot{\rho}_{bb} = \rho_{bb}/T_{1b} + \frac{i}{\hbar}(V_{ab}\rho_{ba} - V_{ba}\rho_{ab}) \tag{6b}$$

$$-\dot{\rho}_{ab} = \{\frac{1}{T_2} + \frac{1}{2}(\frac{1}{T_{1a}} + \frac{1}{T_{1b}})\}\rho_{ab} - \frac{i}{\hbar}(\rho_{aa} - \rho_{bb})V_{ab} \tag{6c}$$

This illustrates the difference in the observed decay if one monitors the polarization component (ρ_{ab}) or population difference ($\rho_{aa} - \rho_{bb}$) of the excited ensemble.

Tang and Satz[4] proposed that an optical transient nutation in CO_2 might be observed when a step-function of light pulse was passed through the medium. Optical nutation is the damped oscillation (mainly by T_2) seen in an intense, transmitted coherent beam due to molecules being driven coherently between the ground and excited state at the Rabi frequency give by

$$\omega_R = \frac{\mu \cdot E}{\hbar} \tag{7}$$

where μ is the transition dipole moment and E is the electric field of the light. Hocher and Tang[5] later observed this in a rotational-vibrational transition in SF_6.

In 1971 Brewer et al.[6] introduced a Stark-switching technique that allowed them to rapidly switch molecular ensembles in and out of resonance with a laser of fixed frequency. By this technique they were able to observe optical nutation, photon echos, and free induction decay (FID).* The obvious limitation of this technique is that the system studied requires a permanent dipole moment.

Telle and Tang[7] demonstrated an electro-optic device that modulates laser frequency with applied voltage. Brewer and Genack[8] placed an

---

*FID is the decay of the electric dipole radiation of an ensemble of coherently excited molecules in the absence of a resonant field. In the Stark-switching technique, one switches between ensembles and the FID appears as a heterodyne signal on top of the slowly varying nutation signal on the ensemble just being excited.

electro-optic device intracavity in a cw dye laser allowing them switch laser frequency with applied voltage pulses. They observed forward coherent transients of $I_{2(g)}$.

Utilizing the same laser frequency switching technique, we reported[9] the coherent optical ringing (COR) and right angle* incoherent resonance decay (IRD) of gaseous I_2 and solid pentacene in p-terphenyl.

---

*By right angle we mean perpendicular to the exciting laser beam.

B. Experimental

These experiments utilize the electro-optic, frequency switching of a single mode, tunable dye laser.[7,8] A Spectra-Physics Model 170 argon ion laser (all lines) is used to pump the free-flowing, horizontal jet stream of Rhodamine 6G in ethylene glycol, of a modified Spectra-Physics Model 580A dye laser. In the dye laser, which normally contains three intracavity etalons for very narrow band (~6 Mhz), single mode output, we added a specially designed, ADP (ammonium dideuterium phosphate), electro-optic device (Lasermetrics). The crystal is oriented such that a medium voltage pulse (10-100 V) changes the dispersion by modulation of the refractive index, thus causing a change in laser frequency proportional to the pulse voltage. While the exact dispersion is critically dependent of the orientation in the cavity (as is mode quality), typical dispersion is ≈1.4 Mhz/V. The switching is clearly demonstrated in Figure 1. Optical alignment and achievement of the desired wavelength were quite difficult, but single TEM_{00} output of 90 mW, vertically polarized, could be achieved.

Figure 1 shows a schematic diagram of the final experimental set-up. A small portion of the beam was split with an uncoated beamsplitter (4% each face). One reflection was sent to a calibrated 1/2 m Jarrel-Ash spectrometer, equipped with RCA IP28 photomultiplier whose anode was connected to a digital voltmeter. This allowed wavelength determination within ± 0.5 Å. More accurate wavelength adjustment was later made by observing the sample fluorescence. The other reflection was directed to

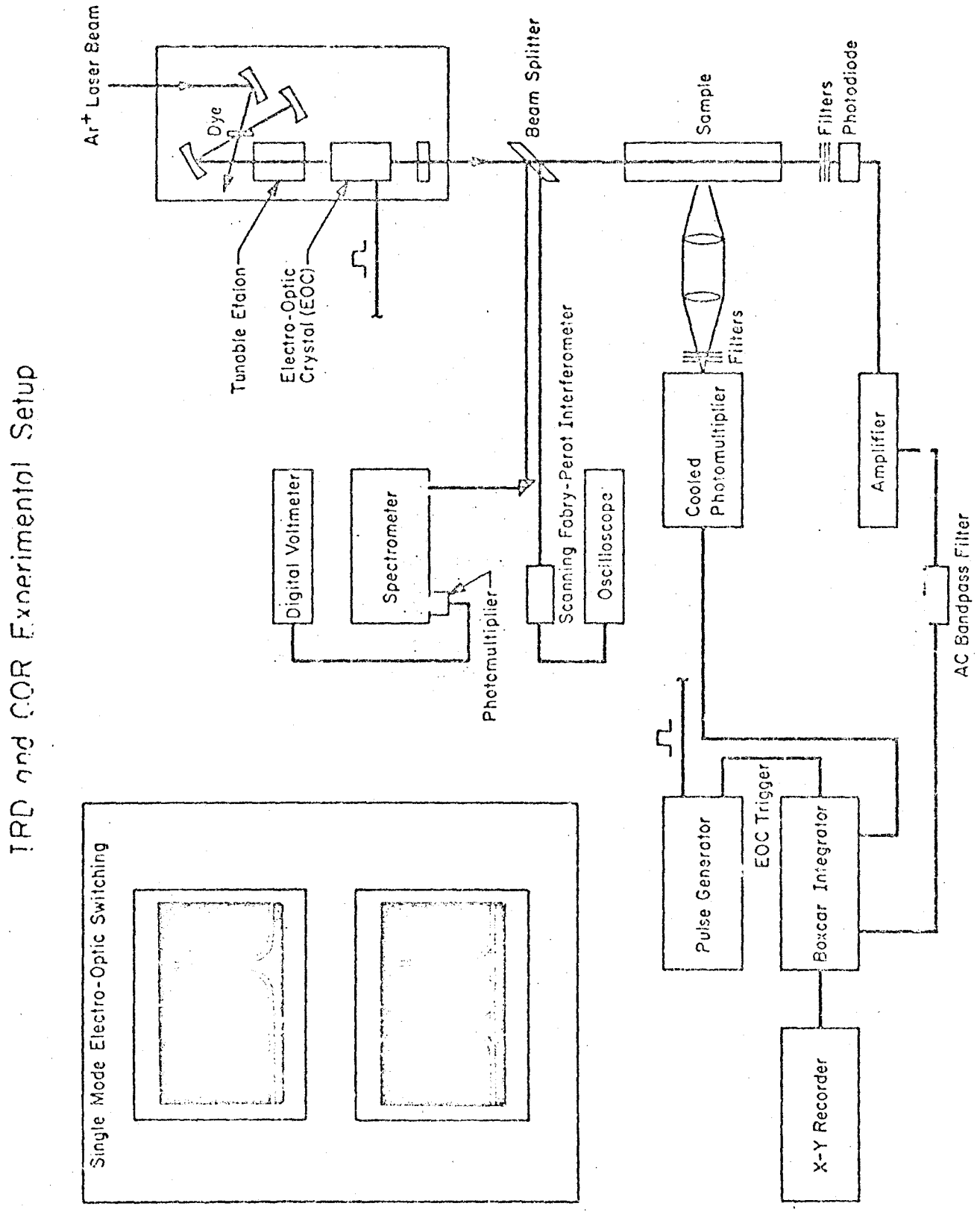
TRD and COR Experimental Setup
Ar+ Laser Beam
Dye
Tunable Etalon
Electro-Optic Crystal (EOC)
Beam Splitter
Sample
Filters
Photodiode
Digital Voltmeter
Spectrometer
Photomultiplier
Scanning Fabry-Perot Interferometer
Oscilloscope
Cooled Photomultiplier
Filters
Amplifier
AC Bandpass Filter
Single Mode Electro-Optic Switching
Pulse Generator
EOC Trigger
Boxcar Integrator
X-Y Recorder

Figure 1

a scanning Fabry-Perot Interferometer (Spectra-Physics Model 476) with a free spectral range of 2 Ghz and an approximate finesse of 200 corresponding to a bandwidth of 20 Mhz. The output of the photodiode backing the interferometer was displayed on an oscilloscope (Fairchild Instruments Model 701) for a continuous display of the mode frequency spectrum.

For the gas phase experiments, the beam was directed unfocused to a 10 cm cylindrical sample tube with flat optical windows. A cold finger on the side of the tube was used with a variable temperature bath to control the pressure in the cell. For the COR experiments, the transmitted beam was attenuated and focused on a fast risetime (<1 nsec) Hewlett Packard 5082-4203 photodiode, reverse biased to 15 V. The output was amplified with a Princeton Applied Research Model 115 amplifier, past through an AC highpass filter, and to a PAR Model 162 Boxcar Integrator with Model 164 gated plug-in. The boxcar was triggered from the pulse generator (HP Model 214) driving the electra-optic crystal. The averaged signal was sent to an HP Model 7590 x-y plotter for permanent record.

For the IRD experiment, the fluorescence is collected and focused onto an EMI 9558 photomultiplier in a cooled (-78°C), rf and magnetically shielded housing. The photomultiplier signal is likewise sent to the boxcar integrator. A sharp cutoff optical filter was used to remove the scattered laser light.

For the solid state experiments, an optically thin sample, sliced from a single crystal grown from a melt by the Bridgeman technique, was

mounted in the tail of an optical liquid helium dewar (Kontes-Martin). The crystal was cooled very slowly to prevent cracking. Following helium transfer, the dewar is pumped (Sergeant-Welch Model 1374) below the λ-point of liquid helium to eliminate scattering from bubbles and reduce phonon population. As the dewar has three windows, both the transmitted beam and right-angle emission can be monitored.

We should note at this point that the extreme requirements on laser stability and the high frequency and low amplitude of the signals make these experiments very difficult indeed. Not until we moved the laboratory downstairs to a carefully temperature-controlled room and covered the laser with an insulated box to minimize acoustic and thermal fluctuations was the laser sufficiently stable. During the development of the technique, many electronics problems, such as cable reflections and ground loops, had to be carefully traced to their source and eliminated or shielded. As these high frequency, low amplitude electronic transients resemble the signal we were searching for, a detailed routine of diagnostic procedures were developed to distinguish between them.

Iodine used in the experiments was commercial material (Mallinkrodt), freeze-degased and sublimed into the sample cell. Pentacene (Aldrich) was twice sublimed. P-terphenyl (Adrich) was zone refined (~100 passes) and only the center portion of the sample was used.

C. Demonstration of Coherent Transients in Gases and Solids

I_2 represents a prototype system as the COR experiment was also done by Brewer and Genack[8] and we can expect a minimum amount of vibronic scrambling. The gas was excited at 5897.5 Å ($X\,^1\Sigma_g^+ \rightarrow B\,^3\Pi_{0^+u}$) and Figure 2 shows the IRD on and off resonance with the transition, the optical nutation, and the voltage pulse to the electro-optic crystal for a pressure of 105 torr (0°C). The IRD yields a decay of 0.23 μsec. The total decay can be partitioned into a radiative part and a part due to deactivating collisions. Stern and Volmer[10] have shown how the later depends on pressure. From our results, we extract a radiative lifetime of 7.5×10^{-7} sec, in good agreement with literature values.[11] The experiment was tried at room temperature (very strong emission) and 77°K and no signal was seen.

The FID of I_2 at 0°C is shown in Figure 3. The FID decay can be shown[12] to be

$$\frac{1}{\tau} = \frac{1}{T_2} + \left[\frac{1}{T_2^2} + \left(\frac{\mu \cdot E}{\hbar}\right)^2 \frac{T_1}{T_2}\right]^{1/2} \qquad (8)$$

By extracting the Rabi oscillation frequency from the optical nutation and T_1 from the IRD, one solves for a $T_2 \simeq 1 \times 10^{-7}$ sec.

Recently, this experiment has been performed in a collisionless molecular beam[13] yielding $T_1 = T_2 = 1.24 \pm 0.02$ μsec as expected.

As mentioned, we now have a way of extracting the transition dipole moment μ. The optical nutation, Figure 2, is at the Rabi oscillation frequency as defined in equation 7. By measuring the laser power and

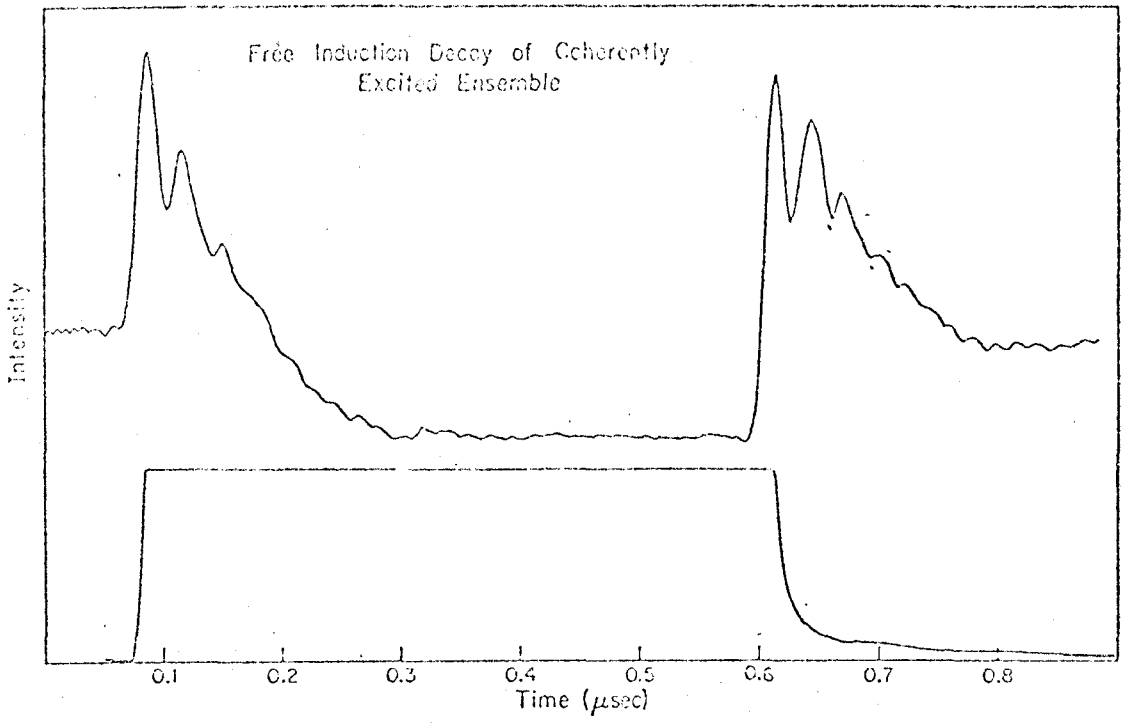

Figure 3

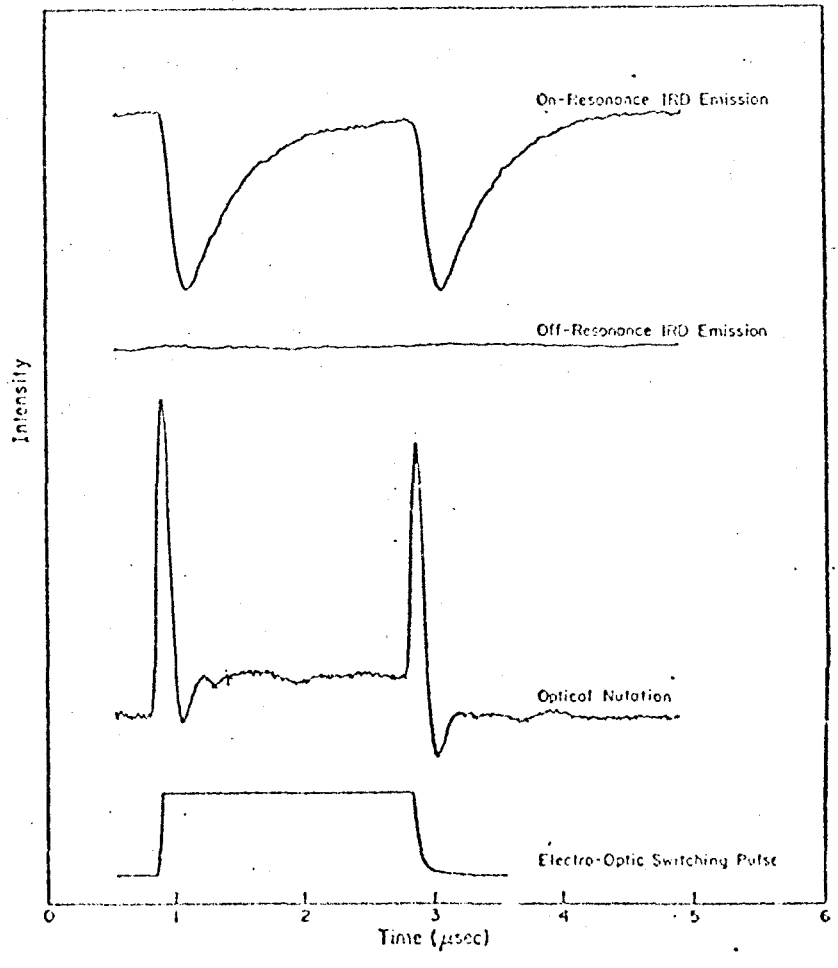

Figure 2

beam diameter, we get $\mu = 0.05$ debye for $I_2(X^1\Sigma_g^+ \rightarrow B^3\Pi_{0_u^+})$.

Pentacene, as a guest in a p-terphenyl host, has been shown to occupy four distinct sides[14,15] with a linewidth of 1-3 cm^{-1} at 1.8°K. The optical nutation[9] from excitation into the 0_1 origin (5921.7 Å). FID was not observed because it is too fast for our detection system. From this data we extract a crude value of $\mu \simeq 0.25$ debye. From the dispersion of the electro-optic crystal and the voltage required to see nutation, we find a homogeneous linewidth of ~40 Mhz.[16] This is in contrast to the much broader lines observed before.[14,15] The significance of this is that now the linewidth characteristic of the actual dynamics (i.e., exciton-phonon coupling and nonradiative decay) is available. A systematic study of the temperature dependence as well as investigation in a collisionless molecular beam are now underway to probe these dynamical processes.

We have demonstrated here techniques that allow us to extract both T_1 and T_2 information on a time scale ≥10 nsec. For highly allowed transitions or systems where the damping processes are much larger, decay is likely to occur on a picosecond time scale. In the following section we describe techniques we hope will allow us to extend our observation of coherent transients to the picosecond regime.

II. Picosecond Coherent Transients and Time Resolved Absorption Spectroscopy

A. Introduction

When, in 1965, the saturable absorbtion of certain organic dyes was used to Q-switch and mode-lock solid state lasers,[17,18] a new domain of time resolution was opened to the scientist. As the accuracy of any measurement can only be as good as the unit of measure, the availability of picosecond (10^{-12} sec) pulses provided a new "yardstick" with which fundamental events could be probed.

Since then, the development of time resolved spectroscopy has centered on the development of the mode-locked Nd:glass laser or flash-lamp pumped dye laser. While the high power available from these sources makes them attractive for many experiments, the pulse-to-pulse and shot-to-shot irreproductability as well as the time delay between shots has often dictated the selection of a single pulse from each train for accurate measurement--a clumsy and time consuming affair for many experiments. In addition, the lasing wavelength of the Nd systems (1.06μ) requires frequency doubling in non-linear crystals, an inherently inefficient process, to provide radiation capable of probing the electronic structure of molecules. The recently developed passive mode-locked, "cw" dye laser,[19,20] characterized by a stable, reproducible, continuous output of picosecond and even subpicosecond pulses, combines picosecond resolution with the signal averaging advantages of a cw experiment.

To date, most picosecond experiments have concentrated on time resolved fluorescence of liquids and solutions.[21] The high power of a glass system is required for this as is very fast detection, such as a streak

camera. However, many experiments, particularly those probing radiationless processes, cannot be done this way as the details of the process in question do not manifest themselves in the emitted light. An alternative procedure is to use a preparation pulse/probe pulse technique commonly used by Kaiser et al.[22] Our version of this technique, time resolved absorption spectroscopy, will be detailed later on.

To our knowledge, only two picosecond experiments have been published in solids. Solids not only offer the opportunity to study an "isolated molecule" (low concentration mixed crystal) at low temperature (1.7°K) where vibrational complications are minimized, but the entire field of excitation dynamics and energy transfer in these systems lends itself nicely to picosecond experiments. Lauberau et al.[22] have measured the decay of hot TO phonons in diamond, while Alfano and Shapiro[23] have measured the optical phonon lifetime in calcite.

Our interests center on the optical electronic structure of solids. We are particularly interested in understanding the various radiative and nonradiative processes that contribute to the homogeneous linewidths of excited states as well as the precise time evolution of such states. In Section I of this report, a description was given of new techniques we developed to allow us to routinely measure true homogeneous linewidths and, by varying parameters such as pressure or temperature, gain insight into the contribution of collisions in gases or phonon population in solids. However, these experiments are limited to a time resolution of ca. 10 nsec.

With the laser we have built, detailed in the following section,

time resolution of ca. 1 psec is attainable. With such resolution, we can not only monitor the time evolution of an excited state but we believe by the method described in Section C that we will be able to measure ultra-fast dephasing times (T_2) as well.

B. Experimental

We have constructed a passively mode locked, cw, tunable dye laser. Such lasers have been built in a variety of configurations.[19,20,24] Figure 4 illustrates schematically our seven mirror, three beam-waist, astigmatically compensated cavity.

A Spectra-Physics Model 170-00 argon ion laser (all lines) is used to pump a vertical free-flowing jet stream of rhodamine 6G chloride (Exciton Chemical Company) in ethylene glycol (3×10^{-3} M). The argon laser and all dye laser components, except the circulation systems, are mounted on a Newport Research Corporation vibration isolated optical table. Components on the table are covered with a lucite box for protection from dust. The vertical polarization of the Ar^+ laser is rotated (NRC beam steering device) and directed to the input coupling mirror (LEI broadband high reflectance) and focused into the dye jet. Pump powers as high as 18 W are available, although typical pump powers are 4-5 W (40 amps, 450 V).

The dye circulation system, shown schematically in Figure 5, equipped with Weldon S-105 variable speed pump, 0.8 μ filter and Spectra-Physics nozzle (Model 375 dye laser) is capable of pumping speeds of approximately 8 m/sec without cavitation in the jet. The dye reservoir is externally cooled to room temperature to minimize dye decomposition. The nozzle and collector are mounted on a Line Tool Company x-y-z micropositioner for optimum positioning in the beam waist. The nozzle can also be rotated while in operation to assure orientation at Brewster's

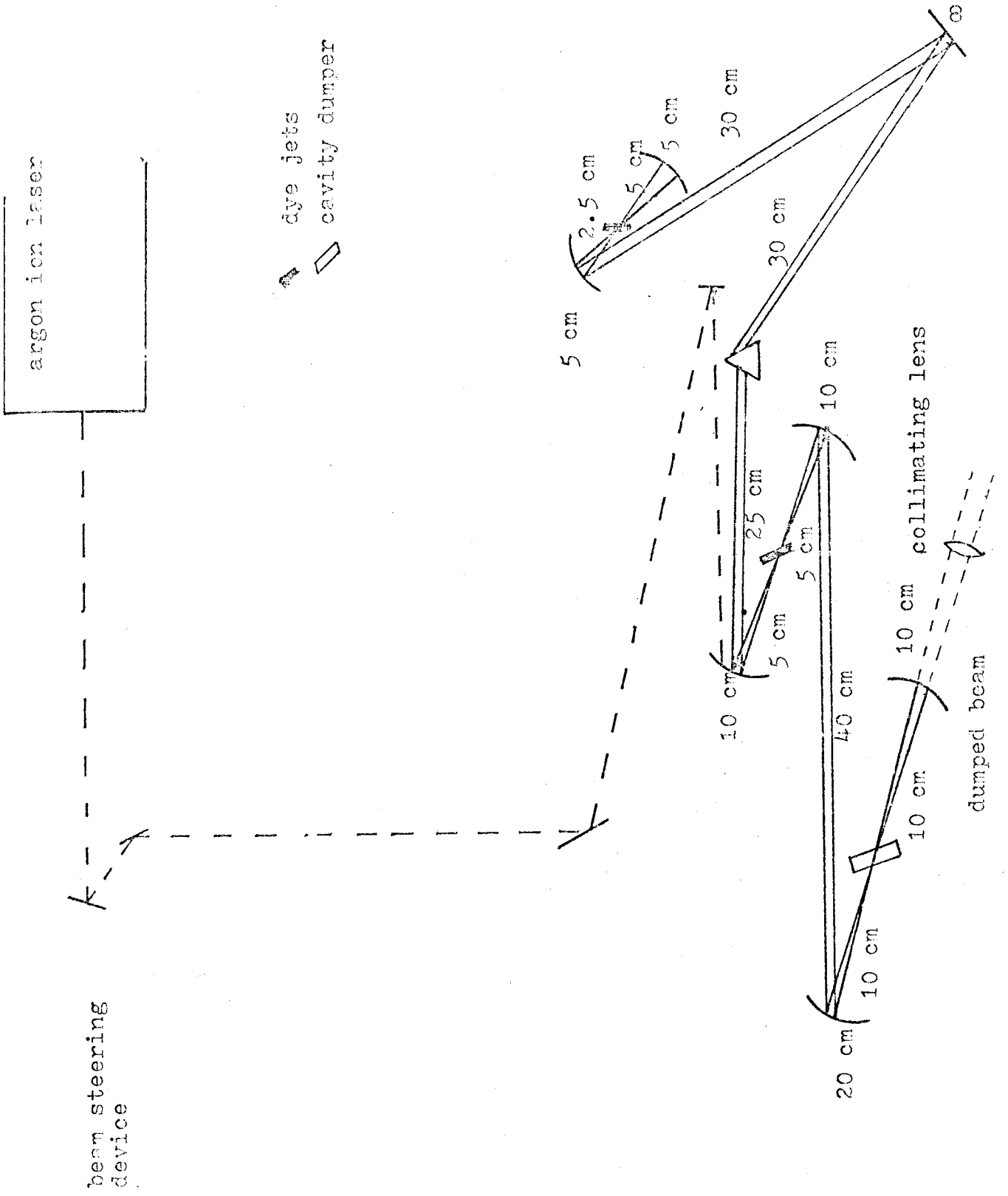
argon ion laser
dye jets
cavity dumper
beam steering device
2.5 cm
5 cm
5 cm
5 cm
30 cm
30 cm
∞
10 cm
25 cm
5 cm
5 cm
10 cm
40 cm
20 cm
10 cm
10 cm
10 cm
10 cm collimating lens
dumped beam

FIGURE 4

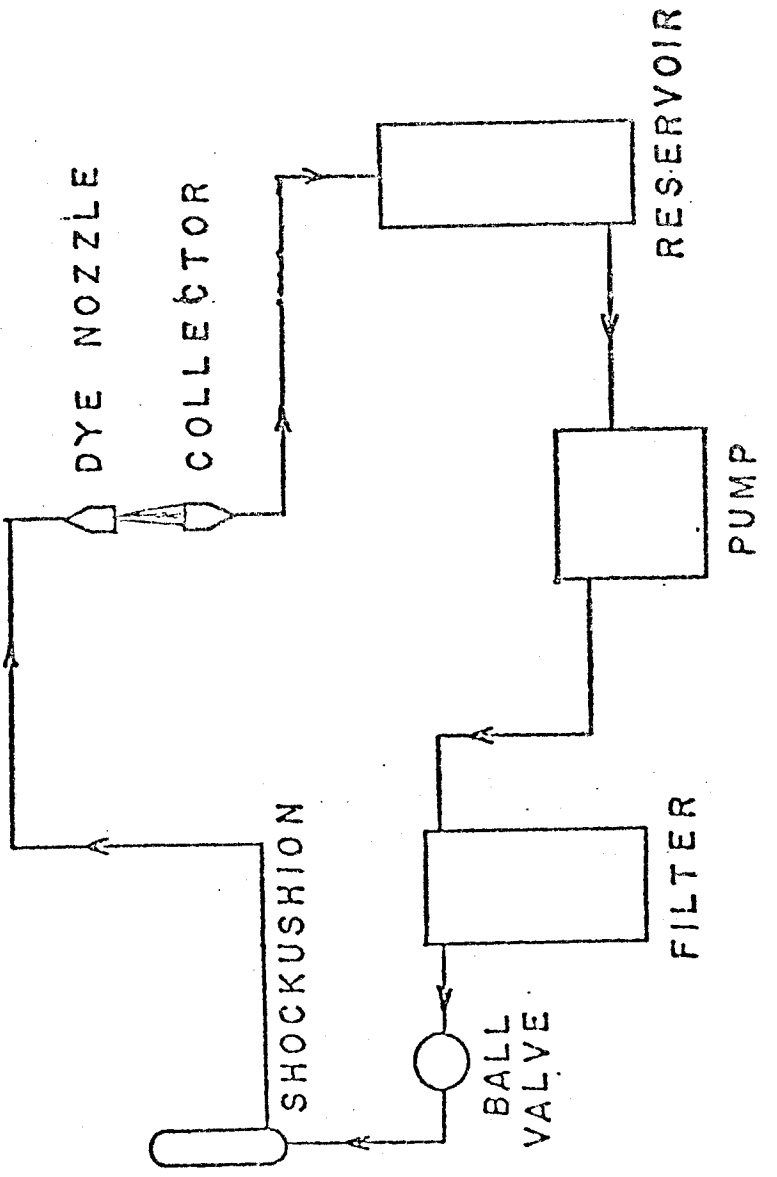

DYE FLOW

FIGURE 5

angle to the lasing path.

The cavity utilizes LEI high energy mirrors (>GW/cm^2) in modified Lansing Research Corporation 2" mounts. Key mirrors are mounted on micrometer translators for optimum cavity length adjustment.

Experimentally, alignment of the cavity required the most effort. Originally, a four mirror cavity was got to lase in order to acquaint ourselves with the important alignment parameters of the confocal mirror arrangement around the jet. The threshold (minimum pump power required for lasing) was minimized at this configuration and we then proceded to a six and finally to the seven mirror cavity. While time consuming, this step-wise increase in cavity complexity was necessary in order to allow us to develop a systematic procedure for cavity alignment.

The procedure developed was an iterative one involving alternate adjustments of mirror tilts and cavity length. After rotation of polarization, the argon ion laser beam is directed into the cavity via two plane mirrors indicated schematically in Figure 4. The beam was very carefully adjusted to be parallel to the table surface and its height from the table established the height of the plane in which the laser would oscillate. The argon beam was directed to the input mirror approximately one half the radius from the center, and the dye stream was located at its focus (by eye).

Next the 10 cm cavity end mirror was removed and replaced by a lens of the same focal length through which a He-Ne alignment laser was directed. The He-Ne laser had been adjusted parallel with the table surface and to the correct height. The He-Ne beam was then directed

through the entire cavity. Its height was measured before and after each mirror to allow adjustment of the vertical tilt of each mirror and ensure lasing would be in a plane parallel to the table surface. The beam was made to go through the fluorescent spot (due to the argon ion laser) in the jet and directed on a complete round trip through the cavity and back on itself.

Next, the end mirror was replaced and the argon ion power increased to ~4 W. At this power, a number of bright, fluorescent spots were visible at the plane cavity mirror. Their sizes were determined by the distances of the various confocal mirror pairs. It should be noted that the beams here are not perfectly collimated and, in fact, slightly convergent beams are required to achieve lasing. The appropriate fluorescent spot sizes, indicative of the appropriate convergence, were determined empiracally by trying hundreds of combinations, and these were adjusted appropriately.

Changing the path length changes the round trip path such that the He-Ne laser was again coupled into the cavity and made to come back on itself following a round trip. Care was paid that it hit approximately in the center of all the mirrors and intersected the jets in the center. The end mirror was again replaced and the power increased. By watching the overlap of the fluorescent spots on any mirror while adjusting the two cavity end mirrors, lasing could be achieved.

Following the initial lasing of the full cavity, there was a period of several weeks where we became familiar with it and effort was made to reduce the threshold. It is important to have a low threshold before

attempting mode locking. With a high threshold, hence high intracavity power, the mode locking dye apparently saturates and no pulses are seen. Before attempting mode locking, the threshold was reduced to ~900 mW with a tuning range of approximately 5850-6200 Å.

Mode locking was achieved by the slow addition of the saturable absorbing dye, 3,3'-diethyloxadicarbocyanine iodide (DODCI), to the second free-flowing jet stream of ethylene glycol. The dye was dissolved in methanol at high concentration and added dropwise to the ethylene glycol reservoir, allowing ample time for mixing. At DODCI concentration, $<10^{-5}$ M modulation of the laser output was seen. The dye has the characteristic of non-linear absorption. That is, its absorption decreases with increasing intensity. Thus, the dye discriminates against low intensity cw oscillation in favor of high peak intensity, short pulsed oscillation. Measurements of the photobleaching recovery time of DODCI vary from 10-250 psec, depending on the experimental conditions. However, no clear demonstration has been made as to how pulses as short as 1 psec are generated, although there is a fair amount of theoretical work in this area.[25-27]

Using DODCI at an optimum concentration of ~3 x 10^{-5} M, pulses as short as 0.9 psec have been achieved.[20a] Addition of the dye Malachite Green, which has a very fast recovery time, generates pulses as short as 0.5 psec, although these pulses have been shown to be frequency chirped.[20b] Compression in time by use of a grating pair has realized pulses of 0.3 psec.

The laser output is monitored via the small transmittance of one of

the cavity mirrors focused on a fast diode detector.[13] The photodiode is an HP 5082-4220 built in a special mount and reverse biased to 150 V, yielding a risetime of ~200 psec. The signal is fed to a Textronix Type 1S1 sampling unit in a Type 547 oscilloscope for a combined resolution of ~400 psec. Figure 6 shows the detection limited pulses.

Mode locked glass lasers and cw dye lasers commonly use a slightly transmitting mirror in order to couple 2-5% of the available power out of the cavity. As our system is of inherently lower power than a glass system, in order to increase our output power we employ an alternate method. In the third beam waist a Spectra-Physics Model 365 acousto-optic cavity dumper is placed.[29] The dumper is an ~1 cm^3 quartz crystal, oriented at Brewster's angle, upon which has been sputtered a zinc oxide transducer. The transducer, powered by a gated 470 Mhz oscillator, pulses a traveling acoustic wave in the quartz crystal. The acoustic wave serves to induce the equivalent of a diffraction grating in the crystal by creating alternate areas of higher and lower refractive index. The laser pulse is "diffracted" out of the crystal. We have been able to couple ~50% of the intracavity energy out of the cavity at a repetition rate of 10^5-10^6 sec^{-1} without damping oscillation. Figure 6 shows the dumped pulses and the subsequent build up of the cavity energy. Triggering is achieved by taking the output of our photodiode monitor into a Textronix 454 oscilloscope. Approximately 100 pulses are displayed on the CRT and the "gate A out" of the scope is used to trigger another pulse generator. In this way we get one pulse for every 100 laser pulses. The triggered pulse generator (Rutherford Model B16) is used to gate the

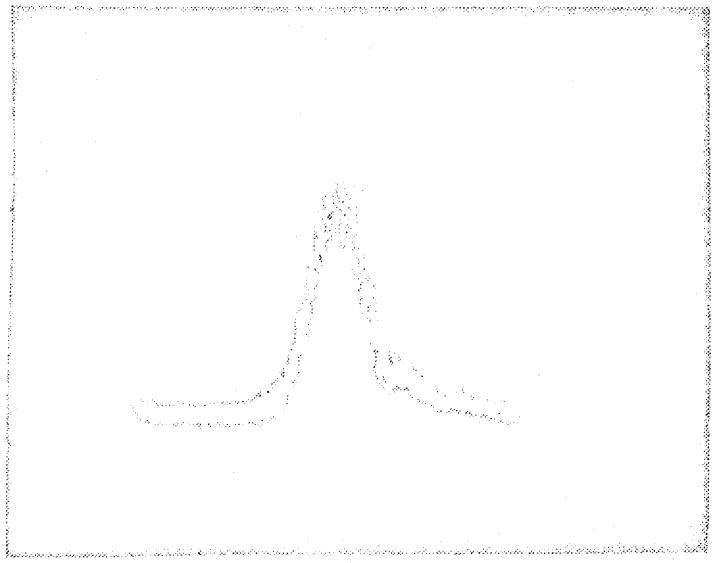

single pulse
FWHM = 400 psec
detection limited

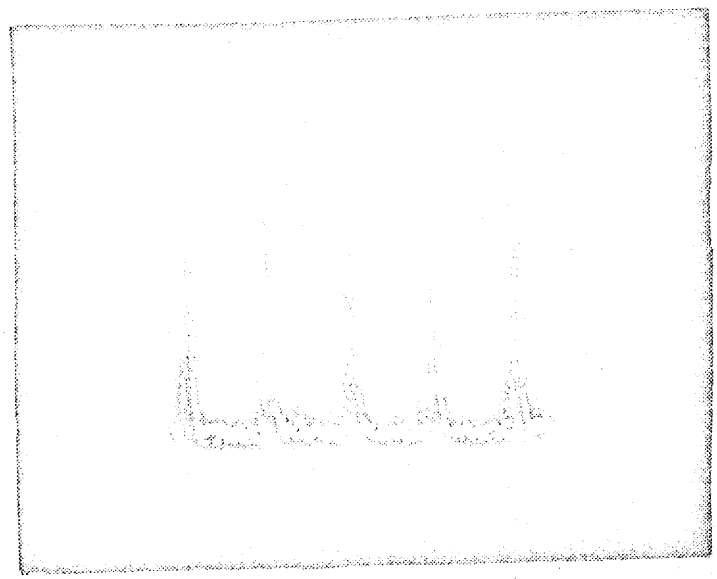

pulse train,
period = 10.4 nsec
corresponding to a
cavity length = 156 cm

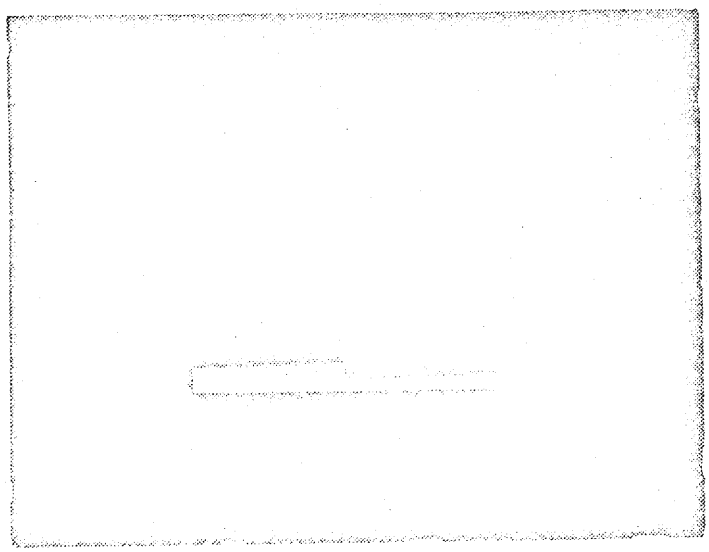

pulse train showing
point of dumping
and cavity buildup

FIGURE 6

rf oscillator powering the dumper. The pulsewidth and delay of the pulse out, relative to the trigger pulse in, are adjustable at the pulse generator for maximum dumped power and synchronization. Changing the time base of the oscilloscope changes the repetition rate of the dumped output.

Utilizing this laser time resolved absorption experiments require a preparation pulse/probe pulse technique. The set up for this is shown schematically in Figure 7. An output pulse from the laser is beamsplit into two components of approximately 90% and 10%. The more intense portion is directed through a fixed optical delay of approximately 70 cm. The weaker portion is directed to a variable delay of the same length and the pulses directed parallel to a lens where they are focused to the same spot in a sample. The variable delay is controlled by a high precision stepper motor run translator (Klinger Scientific Model MT 160). By scanning the variable delay, one delays the weaker or probe pulse relative to the more intense or preparation pulse. As the pulses are coming at a high rep. rate, one can scan the delay very slowly and signal average at each point. By measuring the attenuation of the probe pulse as a function of the delay, one maps out the time resolved absorption spectrum. The system can step in increments of 10 μ which corresponds to a time delay of 6.6×10^{-14} seconds with reproducibility within 1 μ. Hence, the resolution of the system is only limited by the pulsewidth. For high intensity signals, the light is detected with an RCA IP28 photomultiplier and sent directly to an x-y recorder. The x-axis drive of the recorder is provided by a ramp from our programmable stepper

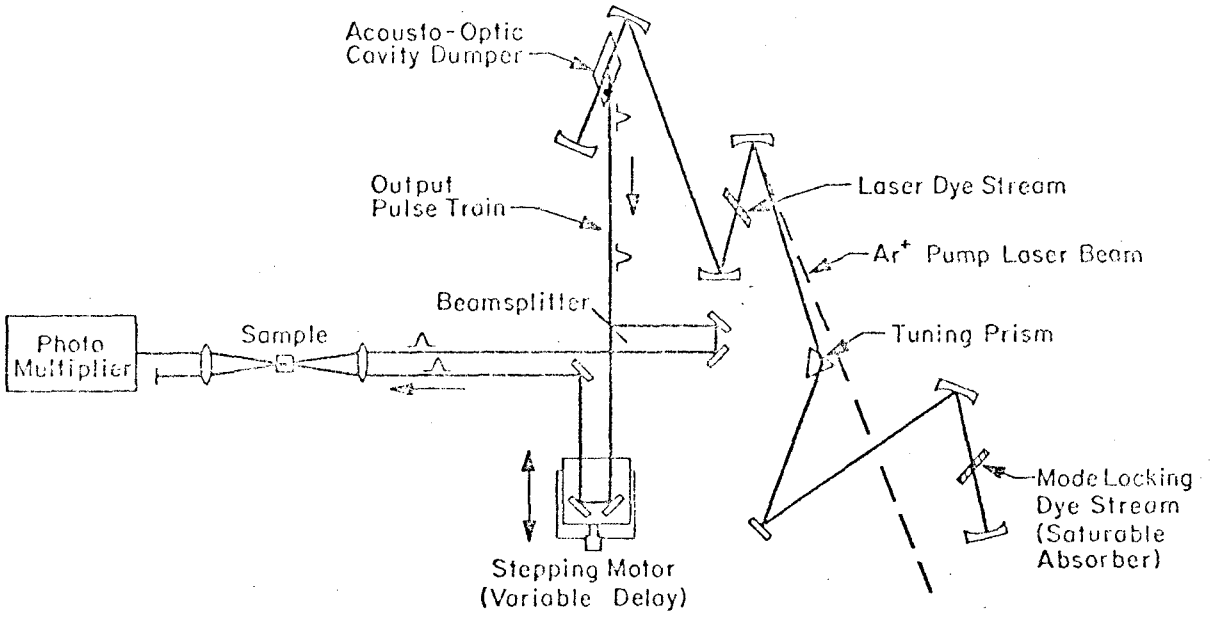

Subpicosecond Mode Locked Dye Laser

FIGURE 7

motor controller (Chemistry Department Electronics Shop). In the event of low level signals, single photon counting techniques will be used. Light is focused onto a high sensitivity, low noise, RCA C31034 A photomultiplier housed in a cooled (-78°C), rf and magnetically shielded housing (Products for Research). The PMT is biased to -2000 V by a Victoreen Model 1HVN high voltage supply.

The signal is carried through a double-shielded cable and terminated into 50 ohms at an EG and G counting module. The signal is amplified up to 64 times by AN 101 amplifiers and passed into a TR 104S discriminator set to maximize signal to noise. The output of the discriminator, a series of standard pulses, is fed into a Nuclear Data Series 2200 multichannel analyzer (MCA). The channels of the MCA are advanced by the stepper motor controller as the delay is scanned.

To analyze the pulse width, this same configuration is employed with the sample replaced by a thin slice (0.7 mm) of KDP, in a goniometer-type mount. The crystal is cut for angle-tuned phase matching across the region 5800-6300 Å (Cleveland Crystals Inc.). As one scans through the overlap of the pulses in the KDP, the high intensity causes generation of the second harmonic (~3050 Å). One scans the delay, filters out the fundamental, and records second harmonic intensity vs. pulse delay τ. It can be shown [30-32] that a plot of second harmonic intensity vs. τ yields a function $f(\tau)$ given by

$$f(\tau) = 1 + 2G^2(\tau)$$

where $G^2(\tau)$ is the so-called second order correlation function of the

pulse defined by

$$G^2(\tau) = \frac{\langle I(t)|I(t+\tau)\rangle}{\langle I^2(t)\rangle}$$

If one then assumes a pulse shape, the pulse width can be extracted from $f(\tau)$.

Currently, we are in the process of characterizing our pulses via this technique. Following characterization, the experiments detailed in the following sections will be started. As the details of the experimental configuration required are dictated by the experiment, these are included in the following discussion of the specific experiments.

C. Planned Experiments

1. Measurement of Radiationless Transition Rate in Pentacene

The question, "Given an electronically excited molecule, how does it decay or relax," is probably the fundamental question in molecular photophysics. Historically, for an excited singlet state, it has been said that the available decay channels are: emission (coupling with the continuim radiation field); non-radiative internal conversion to a vibrationally excited ground state; non-radiative intersystem crossing to a vibrationally excited triplet state; resonant singlet-singlet energy transfer to another molecule. While the radiative decay routes are seemingly understood, there still exists much confusion in the understanding of the non-radiative decay channels for molecules. In fact, the very language in which the problem has been couched, that of "singlets" and "triplets," "intersystem crossing," "fluorescence" and "phosphorescence," while necessary, has contributed to this confusion by the shaping of our conception of the problem in some misleading ways. It is our feeling that the large scope of theoretical work in this area, when tested by experiments now possible with tunable, coherent light sources, can be unified to provide us with a reasonable description of these fundamental processes.[33]

The time evolution of a discrete excited state in the presence of a coupling continua (phonon field, radiation field, molecular vibrations, etc.) is a well-studied problem.[34] In particular, Bixon and Jortner[35] have treated the coupling with the vibrational manifold of a nearby

electronic state as a model for electronic relaxation. Consider the zero-order system (i.e., no vibronic coupling, no interaction with radiation field) diagrammed in Figure 8. This system, the eigenstates of the so-called Born-Oppenheimer Hamiltonian (H_{BO}), consists of a molecular ground state ϕ_0, excited state ϕ_s with radiative bandwidth Γ_p, and the manifold of vibrational levels ϕ_i with uniform density $\rho = \varepsilon^{-1}$. We will assume ϕ_p carries all the oscillator strength from the ground state. The true Hamiltonian for the system can be expressed as

$$H = H_{BO} + H_V + H_{rad} + H_{int} \tag{1}$$

where H_V is the intramolecular coupling term arising from the nuclear kinetic energy operator, H_{rad} corresponds to the free radiation field, and H_{int} is the matter-radiation interaction term.

In the absence of the radiation field, the molecular eigenstates are superpositions of the quasi-degenerate, zero-order states given by

$$\psi_n = \alpha_s{}^n\phi_s + \sum_i \beta_i{}^h\phi_i \tag{2}$$

In the presence of the radiation field, the eigenstates are superpositions of the first-order states[2] and the continuim of one-photon states $\phi_{E'}$

$$\psi_E = \sum_n a_n\psi_n + \int C_{E'}\phi_{E'}dE' \tag{3}$$

Of interest is the excited state prepared by a short light pulse at $t = 0$. In terms of ψ_E's, it is represented as

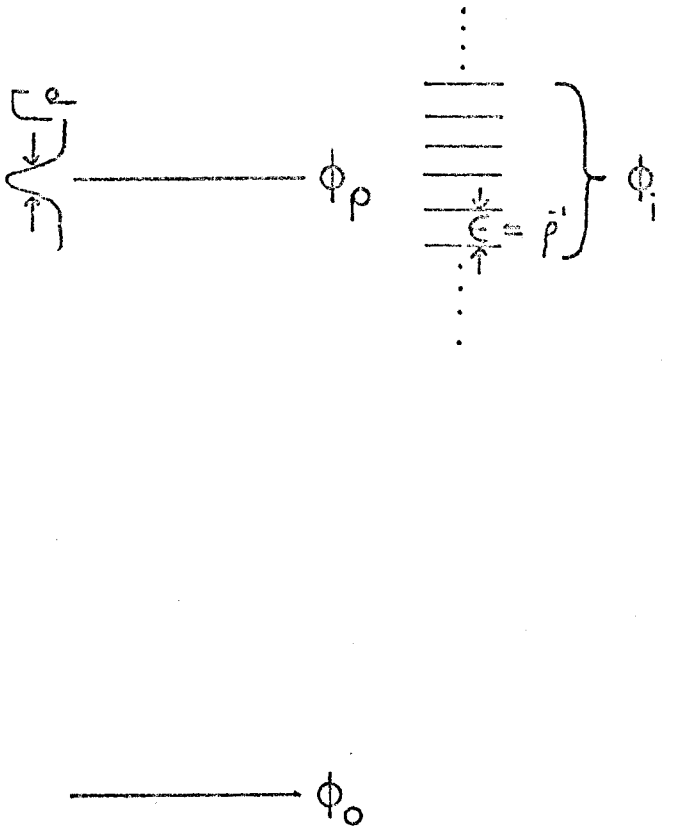

FIGURE 8

$$\Psi(t=0) = \int \langle \phi_o | T | \psi_E \rangle \psi_E dE \tag{4}$$

where T is the transition operator. The transition matrix element in (4) is proportional to the amount of ϕ_s in state ψ_E (as only ϕ_s carries oscillator strength). This amplitude, obtained from (2) and (3), becomes

$$a_s(E) = \langle \phi_s | \psi_E \rangle = \sum_n a_n \langle \phi_s | \psi_n \rangle = \sum_n a_n \alpha_s^n \tag{5}$$

Substituting, this yields

$$\Psi(t=0) = \int \sum_n a_n \alpha_s^n \psi_E dE \tag{6}$$

To examine the time evolution of this state, we need only include the phase development of the individual eigenstates.

$$\Psi(t) = \sum_n \alpha_n^s \int a_n \psi_E \exp(-iE_e t/\hbar) dE \tag{7}$$

At this point, one might ask how we can probe the time evolution of state Ψ. An equivalent question is, how does the amount of ϕ_s, our primary Born-Oppenheimer state, in Ψ evolve in time (i.e., what can we learn about "intersystem crossing?").

The time-resolved absorbtion of a weak probe pulse by our system, following preparation of state Ψ at t = 0 by an intense pulse, is a method by which we can probe the time evolution of $\Psi(t)$. If we assume that the probe pulse is sufficiently weak so as to not perturb the evolution of $\Psi(t)$, then the absorbtion rate is given by:

$$\dot{\alpha}(t) = \frac{2\pi}{\hbar}|\langle\phi_0|T|\Psi(t)\rangle|^2\rho \tag{8}$$

where ρ is the density of radiation field states. Letting $\Gamma/\hbar$ be the absorbtion probability of ϕ_s, given by

$$\Gamma = 2\pi|\langle\phi_0|T|\phi_s\rangle|^2\rho \tag{9}$$

then we can express (8) as

$$\dot{\alpha}(t) = \frac{\Gamma}{\hbar}|A_s(t)|^2 \tag{10}$$

where $A_s(t)$ is the amplitude of ϕ_s in Ψ at time t given by

$$A_s(t) = \langle\phi_s|\Psi(t)\rangle = \sum_n \alpha_n{}^s \int a_n \langle\phi_s|\phi_E\rangle \exp\left(\frac{-iE_E t}{\hbar}\right)dE$$

$$= \sum_{nm}\sum \alpha_s{}^n \alpha_s{}^m \int a_n a_m \exp\left(\frac{-iEt}{\hbar}\right)dE \tag{11}$$

Making use of the appropriate expressions for the coefficients a_n and $\alpha_n{}^s$ and suitably perform the summation (see (19)), we get an expression for $A_s(t)$

$$\frac{2}{=\Pi\Gamma}\int \frac{\exp\left(\frac{-iEt}{\hbar}\right)\{[2(E-E_s)/\Delta]\coth\left(\frac{\Delta\Pi}{2\varepsilon}\right) + \cot\left[\frac{\Pi}{\varepsilon}(E-E_s)\right]\}^2}{1 + (16/\Delta^2\Gamma^2)[(E-E_s)^2 + \Delta^2/4]^2}\,dE \tag{12}$$

where $\Delta = \frac{2\pi v^2}{\varepsilon}$, $v = \langle\phi_s|H_v|\phi_i\rangle$, E is the energy of the ψ_E states, E_s is the energy of the zero-order, primary state ϕ_s, and $\varepsilon = 1/\rho$ is the

spacing between the $\{\phi_i\}$.

Before continuing, it is advisable to point out that the approach outlined here is only one small part of the large volume of work in this area.[33c] This, however, while an instructive example that illustrates the basic approach to the problem, provides us with a framework within which we can discuss the relationship between preparation of a state and its subsequent time evolution.

Let us now consider equation (12) and what simplifications we can make. Bixon and Jortner[35] have treated two cases in detail: the statistical case and the so-called sparse intermediate case. The former is characterized by a very high density of states $\{\phi_i\}$ in the region of ϕ_s such that

$$V >> \frac{1}{\rho} = \varepsilon \tag{13}$$

In this limit, intramolecular relaxation occurs on a time scale

$$t << \bar{h}\rho \tag{14}$$

where $\bar{h}\rho$ defines the Poincaré reoccurance time.

Most large molecules might exhibit a mixed coupling scheme whereby ϕ_s couples strongly with a few active vibrational levels and weakly with a large number of inactive vibrational levels. The former, the sparse intermediate case, is characterized by

$$V > \frac{1}{\rho} \tag{15}$$

The low density of states implies their separation excedes the radiative

bandwidth of ϕ_s

$$\varepsilon >> \Gamma \tag{16}$$

Consequently, with slow intramolecular relaxation, the time scale of the experiment may now excede the recurrance time

$$t > \bar{h}\rho \tag{17}$$

As we shall see, it is this fact that may allow us to see fluctuations in the amplitude of ϕ_s in $\Psi(t)$.

Since,

$$\frac{\pi\Delta}{2\varepsilon} = \pi v^2 \rho > 1 \tag{18}$$

then, in equation (12)

$$\coth \frac{\pi\Delta}{2\varepsilon} \simeq 1$$

Furthermore, we can see that $A_s(t)$ will only be large where $\cot(\pi E/\varepsilon)$ diverges at the points $E = n\varepsilon$, $n = 0, \pm 1, \pm 2....$ Near these points we may approximate

$$\cot\left(\frac{\pi E}{\varepsilon}\right) \simeq \frac{\varepsilon}{\pi(E-n\varepsilon)} \tag{19}$$

Introduction into equation (11) allows us to express $A_s(t)$ as a sum of integrals whose arguments are functions centered about $E = n\varepsilon$. Following

integration and substitution into equation (10), one gets an expression for $\dot{Q}(t)$, the absorbtion rate of a weak probe pulse

$$\dot{Q}(t) = \frac{V^2\Gamma}{\hbar} \sum_{n\leq m} \Sigma(2-\delta_{nm})\cos[(n-m)(\frac{\varepsilon^+}{\hbar})][(n\varepsilon)^2 + \frac{\Delta^2}{4}]^{-1}[(m\varepsilon)^2 + \frac{\Delta^2}{4}]^{-1}$$

$$\times \exp(-(\frac{\varepsilon\Delta\Gamma}{4\pi\hbar})\{[(n\varepsilon)^2 + \frac{\Delta^2}{4}]^{-1} + [(m\varepsilon)^2 + \frac{\Delta^2}{4}]^{-1}\}t) \qquad (20)$$

The absorbtion rate is characterized by two contributions, an exponetial decay and a superimposed cosinusoid with period $\simeq \hbar\rho \simeq 10^{-11}$ sec. Classically speaking, this corresponds to population crossing over into the $\{\phi_i\}$, then crossing back, etc., convoluted with an exponential decay. While the so-called dense intermediate limit has not been worked out in detail, it is anticipated it too may have oscillatory behavior.*

Before considering the proposed experiment designed to probe this excited state behavior, let us examine the question of exactly what state does one prepare and how this influences the time evolution of the system. Very recent work in our laboratory[36] has clearly demonstrated that excited state lifetimes differing by two orders of magnitude result from broad or narrow band excitation of a molecular system.

Following reference 20, consider monochromatic excitation of a

---

*This analysis has not considered the role of phase coherence in the ensemble of excited states. Only recently[37] has the role of T_2 processes in molecular relaxation been considered and it is our hope that experiments detailed in the next section may shed some light on this problem.

molecular eigenstate, as described by equation (2). The time evolution of this stationary state is given by

$$\langle\psi_n|\psi_n(t)\rangle = \langle\psi_n|e^{-iHt/\hbar}|\psi_n\rangle = e^{-iE_n't/\hbar} \tag{21}$$

where

$$\frac{E_n'}{\hbar} = \frac{E_n}{\hbar} - \frac{i}{2}\Gamma^{\text{rad}} - \frac{i}{2}\Gamma^{\text{non-rad}} \tag{22}$$

The relaxation information is contained in the damping matrix elements. Assuming no correlation between decay channels, Γ_n is diagonal and can be expressed as

$$\Gamma_m = |\alpha_s^n|^2\Gamma_p + \sum_i |\beta_i^n|^2\Gamma_i \tag{23}$$

One can see that if the coupling between ϕ_p and $\{\phi_i\}$ is effective, then

$$\Gamma_m < \Gamma_p, \qquad \tau_m > \tau_p \tag{24}$$

and the large molecule will obey the small molecule limit whereby the observed lifetime is <u>longer</u> than the radiative lifetime inferred from oscillator strength measurements.

The broad band excitation prepares a linear combination of molecular eigenstates such as considered by Bixon and Jortner [equation (4)]. δ-function excitation prepares what is essentially the primary state at $t = 0$ since it carries all the oscillator strength:

$$\Psi(t=0) = i\langle\phi_p|\mu\cdot E_o|\phi_o\rangle\sum_n|\psi_n\rangle\langle\psi_n|\phi_p \qquad (25)$$

The probability of finding the system in ϕ_p at some later time t is given by:

$$\mathcal{L}_p(t) = |\langle\phi_p|e^{-iHt/\hbar}|\phi_p\rangle|^2 = |\sum_n|\alpha_s{}^n|^2\ e^{-iE't/\hbar}|^2$$

As $\Psi(t)$ is mostly ϕ_p, it will effectively decay by $\Gamma_p{}^r$ and $\Gamma_p{}^{nr}$, thus giving lifetimes indicative of the primary Born-Oppenheimer state.

Without going into the details of the experiment,[36] the lifetime of pentacene in p-terphenyl[37] was measured at 1.7°K. While pentacene is a large molecule with 102 fundamental vibrations, it exhibits a mixed coupling scheme as described earlier whereby only certain vibrations built on the first excited triplet state can actively couple to the first excited singlet state (the primary state in question). Broadband excitation yielded a lifetime of approximately 90 nsec while narrowband excitation yielded a lifetime of approximately 30 μsec.

We propose to measure the primary state decay (both radiative and non-radiative channels) of pentacene in p-terphenyl at low temperature with picosecond resolution, utilizing our "cw" picosecond dye laser detailed in the previous section. Our short, approximately transform-limited pulses should prepare ϕ_p such that any features in the decay, such as oscillations predicted by the Bixon-Jortner model, should be seen. In as much as the detailed theory for those processes is difficult to evaluate experimentally, time-resolved observation of such

phenomena is very important.

The experimental configuration utilizes the preparation-probe-pulse technique mentioned earlier and is represented in Figure 4. The first intense pulse excites the system into ϕ_p. The probe pulse, slightly delayed in time, samples the population difference between the ground and excited states. By varying the probe pulse delay, one maps out the time resolved absorbtion curve.

2. Picosecond Spontaneously Detected Photon Echo

The photon echo,[2] the burst of light produced when a dephasing ensemble of two-level electric dipoles are made to rephase, is a clear demonstration of the coherence properties of excited states. Experiments of this type allow one to measure T_2, the characteristic dephasing time of the system, the inverse of the homogeneous line width, directly. However, the detection of such a signal is quite difficult as it follows the two intense preparation pulses ($\pi/2$, π) that can easily overload the detector. Recently, our laboratory has reported[39] the first observation of a spontaneously detected photon echo. By this we mean a technique, utilizing a three-pulse sequence, which converts the refocusing polarization to a change in excited population, whereby the echo is emitted spontaneously and thus can be monitored at right angles to the exciting pulses. We propose, utilizing the "cw" picosecond dye laser already described, to make measurements of coherent transients on a sub-nanosecond time scale.

Of what interest is T_2? This optical analogue of the magnetic

resonance transverse relaxation time gives direct information about optical phase coherence in excited states. Any theory attempting to give the time evolution of excited primary states must contain this phase information. Furthermore, the width and shpae of optical resonances, historically a problem of great interest, is dependent on this information. T_2, as a measure of the loss of this coherence, contains detailed information about phase destroying processes such as collisions (gas), electron-phonon coupling, radiationless transitions, and excitation-impurity state interactions.

As the three pulse echo is well described elsewhere,[39] only the details of the picosecond experiment will be presented here. Since we are not at liberty, except perhaps through great difficulty experimentally,[40] to change our pulse widths, instead we change our pulse intensities to yield the proper echo sequence ($\pi/2$, π, $\pi/2$). As the pulse widths required are determined by the period of the Rabi oscillations, changing the magnitude of the electric field (i.e., pulse intensity) changes the oscillation frequency). Thus, one can determine, given the pulse width and the transition dipole moment of interest, the required laser intensity to correspond to any pulse width such that $(\mu \cdot E/\hbar)t = \pi_1\pi/2)$ where μ is the transition dipole moment and t is the laser pulse width. For pentacene in p-terphenyl with $\mu \simeq 0.25$ debye[41] and a pulse width of 1 psec, a $\pi/2$ pulse requires a peak power density of 1.4×10^{12} W/m^2. For a beam focused to a diameter of 25 μ and a pulse repetition rate of 10^5 sec^{-1}, this is equivalent to an average power of 60 μW.

The experimental configuration is shown in Figure 9. A single pulse from the laser is beamsplit into three pulses of the desired intensity ratios (1:4:1). Because of this, the average power required for the experiment is ≈400 μW. The second and third pulses are variably delayed with respect to the first. The experiment consists of fixing Δ_1 and scanning Δ_2 to get the echo, over an entire range of Δ_1's to get the echo decay. As T_1 of pentacene is ≈90 nsec[27] and is much less than the time between laser pulses, signal averaging can be used.

It is our belief that with picosecond resolution detailed studies of the temperature dependence of T_2 in solids, yielding electron-phonon scattering cross sections, will be possible. Furthermore, coupled with other experiments in our laboratories and those already described, a description of the role of phase coherence in radiationless relaxation can be found.

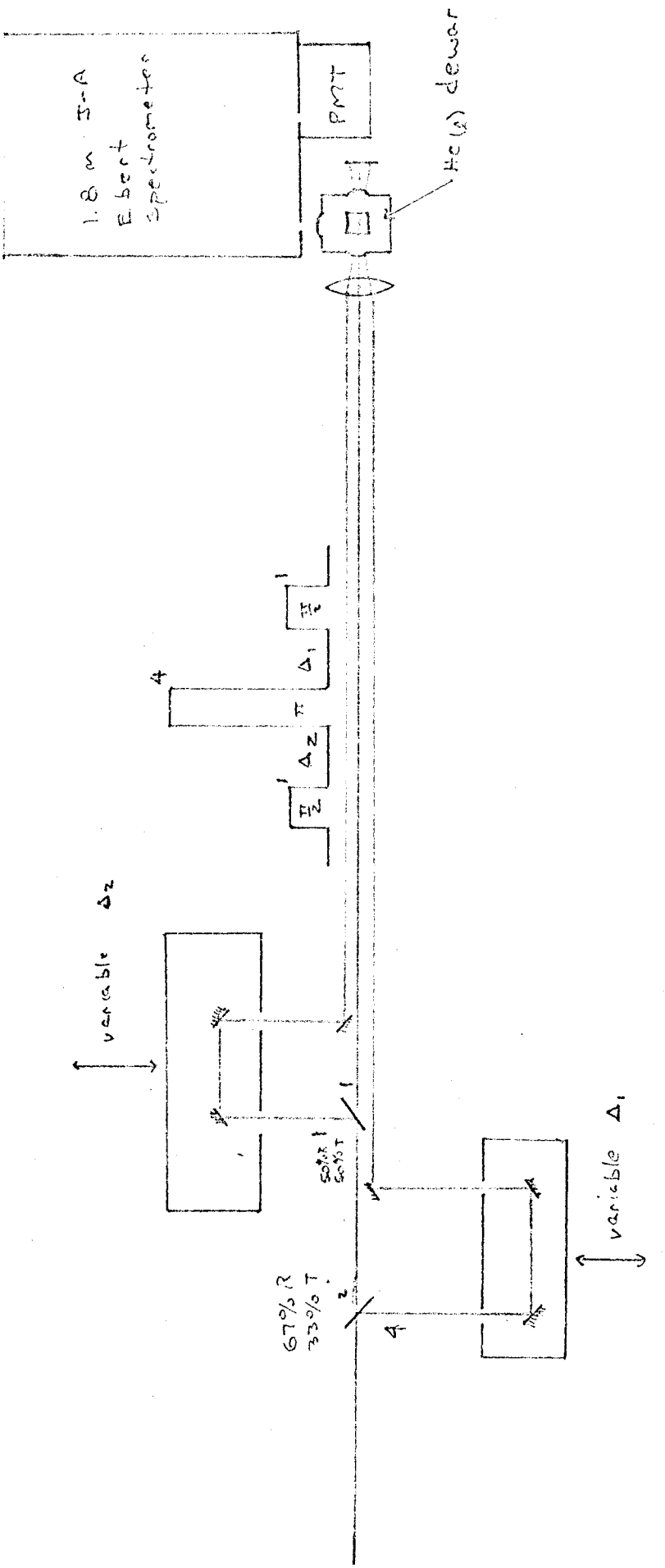
1.8 m f-A
Ebert
spectrometer
PMT
He (a) dewar
F1
Δ1
F
Δ2
F2
variable Δ2
Solar 1
Solar 2
67% R
33% T
variable Δ1

FIGURE 9

III. References

1. E. L. Hahn, Phys. Rev., 77, 297 (1950).

2. N. A. Kurnit, I. D. Abella, S. R. Hartman, Phys. Rev. Lett., 13, 567 (1964).

3. R. P. Feynman, F. L. Vernon, R. W. Hellworth, J. Appl. Phys., 28, 49 (1957).

4. C. L. Tang, H. Satz, Appl. Phys. Lett., 10, 145 (1968).

5. G. B. Hocker, C. L. Tang, Phys. Rev. Lett., 21, 591 (1969).

6. R. G. Brewer, R. L. Shoemaker, Phys. Rev. Lett., 27, 631 (1971); Phys. Rev., A6, 2001 (1972).

7. J. Telle, C. L. Tang, Appl. Phys. Lett., 24, 85 (1974); ibid., 26, 572 (1975).

8. R. G. Brewer, A. Genack, Phys. Rev. Lett., 36, 959 (1976).

9. A. H. Zewail, T. E. Orlowski, D. R. Dawson, Chem. Phys. Lett., 44, 379 (1976); Bull. Am. Phys. Soc., 21, 1283 (1976); T. E. Orlowski and A. H. Zewail, Chem. Phys. Lett., 45, 399 (1977).

10. O. Stern, M. Vollmer, Z. Physik, 20, 183 (1919).

11. L. Brewer, R. Berg, G. Rosenblatt, J. Chem. Phys., 38, 1381 (1963).

12. F. A. Hopf, R. F. Shea, M. O. Scully, Phys. Rev., A7, 2105 (1973).

13 A. H. Zewail, T. E. Orlowski, R. R. Shah, K. E. Jones, Chem. Phys. Lett. (submitted).

14. A. P. Marchetti, W. C. McColgin, J. H. Eberly, Phys. Rev. Lett., 35, 387 (1975).

15. J. H. Meyling, D. A. Wiersma, Chem. Phys. Lett., 20, 383 (1973).

16. A. H. Zewail, T. E. Orlowski, K. E. Jones, Specs. Lett. (in press).

17. H. W. Mocker, R. J. Collins, Appl. Phys. Lett., 7, 270 (1965).

18. A. J. DeMaria, D. A. Stetser, H. Heyman, ibid., 8, 174 (1966).

19. E. P. Ippen, C. V. Shank, A. Dienes, ibid., 21, 348 (1971).

20. a) C. V. Shank, E. P. Ippen, ibid., 24, 373 (1974); b) E. P. Ippen, C. V. Shank, ibid., 27, 488 (1975).

21. For a review, see A. Laubereau, W. Kaiser, Ann. Rev. Phys. Chem., 26, 802 (1971).

22. A. Laubereau, D. von der Linde, W. Kaiser, Phys. Rev. Lett., 27, 802 (1971).

23. R. R. Alfano, S. L. Shapiro, ibid., 26, 1247 (1971).

24. H. W. Kogelnik, E. P. Ippen, A. Dienes, C. V. Shank, IEEE J. Quant. Elec., QE-8, 373 (1972).

25. G. H. C. New, ibid., QE-10, 115 (1974).

26. H. A. Haus, ibid., QE-11, 736 (1975).

27. H. A. Haus, ibid., QE-12, 169 (1976).

28. G. H. McCall, Rev. Sci. Inst., 43, 865 (1972).

29. D. Mayden, J. Appl. Phys., 41, 1552 (1970).

30. D. J. Bradley, H. C. New, Proc. IEEE, 62, 313 (1974) and references therein.

31. C. V. Shank, E. P. Ippen, "Mode-Locking of Dye Laser," Dye Lasers, Vol. 1, Topics in App. Phys. ed. F. P. Schäfer, Springer-Verlag, New York, 1973.

32. H. A. Haus, C. V. Shank, E. P. Ippen, Opt. Comm., 15, 29 (1975).

33. For reviews, see a) S. A. Rice, Excited States, 2, 111 (1975); b) G. W. Robinson, Excited States, 2, 1 (1974); c) K. F. Freed, Topics in App. Phys., 15, 23 (1976).

34. C. A. Langhoff, G. W. Robinson, Mol. Phys., 26, 249 (1973); A. Nitzan, S. Mukamel, J. Jortner, J. Chem. Phys., 60, 3921 (1974); J. M. Friedman, R. M. Hochstrasser, Chem. Phys., 6, 155 (1974) and references cited therein.

35. M. Bixon, J. Jortner, J. Chem. Phys., 50, 3284 (1969); ibid., 50, 4061 (1969).

36. A. H. Zewail, T. E. Orlowski, K. E. Jones, Proc. Nat. Acad. Sci., April 1977 issue.

37. T. E. Orlowski, K. E. Jones, A. H. Zewail, Chem. Phys. (submitted).

38. A. P. Marchetti, W. C. McColgin, J. H. Eberly, Phys. Rev. Lett., 35, 387 (1975).

39. A. H. Zewail, T. E. Orlowski, K. E. Jones, D. E. Godar, Phys. Rev. Lett., in press.

40. E. P. Ippen, C. V. Shank, App. Phys. Lett., 27, 488 (1975).

41. A. H. Zewail, T. E. Orlowski, unpublished results.